PHYSICAL REVIEW A VOLUME 1, NUMBER 6 JUNE 1970

Theory of Intensity-Correlation Measurements on Imperfectly Mode-Locked Lasers

R. H. Picard and P. Schweitzer
Air Force Cambridge Research Laboratories, Bedford, Massachusetts 01730
(Received 3 November 1969)

Intensity-correlation measurements, particularly by the two-photon fluorescence (TPF) technique, have become very popular for determining the temporal behavior of laser emission on a picosecond time scale, although they are subject to considerable difficulties of interpretation. The characteristics of the fluorescent intensity in the TPF technique are analyzed theoretically for two different physically interesting and tractable models of imperfectly mode-locked lasers: (i) a partial-locking model where some of the modes are locked and the rest unlocked, and (ii) a "domain model" where the set of oscillating modes is composed of several perfectly locked subsets randomly phased relative to one another. For each case, the dominant features of the spatial dependence of the fluorescence are calculated analytically, using approximations which are valid for realistic cases involving large numbers of oscillating modes. Computer results for the intensity of the laser field and of the fluorescence are also presented for the domain model. It is shown that the partial-locking model is incompatible with experiment, whereas the domain model is in reasonably good agreement with it. Finally, the dynamical basis of the domain model is discussed.

I. INTRODUCTION

There has been much recent interest in the use of various intensity-correlation methods to determine the temporal characteristics of lasers.[1] These methods are very attractive because, in contrast to standard oscillographic techniques, their resolution is sufficient to measure the expected pulse durations in the picosecond range. In these methods, typically one combines the radiation from the laser with a time-delayed replica of itself and passes the superposition through a medium having a quadratic response to the field intensity. In this paper we consider theoretically the response of such intensity-correlation detectors to the radiation from imperfectly mode-locked lasers. To be specific, we will speak in terms of intensity-correlation measurements by the very popular two-photon fluorescence (TPF) technique of Giordmaine and others,[2] although many of the methods involving second-harmonic generation in nonlinear crystals are mathematically equivalent.[3]

One problem with the use of intensity-correlation methods to obtain information about the intensity is that the intensity-correlation function does not determine uniquely the intensity as a function of time. Moreover, most of the methods, including TPF, yield the intensity-correlation function superposed on a uniform background, resulting from the response of the squaring element to each of the superposed waves acting singly. An unpleasant consequence of these effects for anyone interested in determining whether a laser is emitting picosecond pulses was pointed out clearly by Weber[4] and by Klauder[5]: The TPF trace will have the same qualitative behavior, consisting of regions of enhanced fluorescence on a uniform background, whether the oscillating modes are perfectly locked (resulting in a train of minimum-duration pulses) or completely unlocked (resulting in a randomly fluctuating continuous output). They pointed out that the only difference between the two situations is the peak-to-background contrast ratio of the fluorescence, which is 3.0 in the former case and 1.5 in the latter.[6]

Since the contrast ratios observed in experiments with Nd-glass lasers Q switched by dyes exhibiting saturable absorption [2,5,7] are intermediate between the above values (varying from 1.7 to 2.0), a reasonable step to obtain results consistent with experiment was to combine the two models. Harrach[8] and the present authors[9] considered a partial-locking model for the laser emission in which a portion of the modes are perfectly locked, forming a pulse, and the rest are unlocked, contributing a fluctuating background. Grütter, Weber, and Dändliker[10] considered a model consisting of a combination of random and systematic deviations of the modal phases from the locking condition. They showed that the random deviations contribute a fluctuating background, similar to that in the partial-locking model, whereas the systematic deviations account for the frequency "chirp" postulated by Treachy[1,11] on the basis of his pulse-dispersion experiments.

In the following sections we give more detailed results on the partial-locking model and also consider a new model, the "domain model," in which the oscillating line is divided into several groups, or domains, having perfect internal phasing but random phases relative to other domains. On

the basis of the assumption that the unlocked portion of the field in the partial-locking model behaves like Gaussian noise, we obtain an analytic solution for the TPF contrast ratio as a function of the degree of mode locking, which exhibits a strong dependence on the number of oscillating modes. We also consider the response of a fast photodetector to the partially locked laser field, showing that the ratio of the peak photocurrent to the background photocurrent depends only on the degree of mode-locking and the ratio of two characteristic times. Turning to the domain model, we show that it results in broadened pulses with considerable substructure, and we determine the qualitative behavior of the TPF as a function of position in this model. We also present typical computer calculations of the intensity and of the fluorescence.

Following a brief discussion of TPF measurements in general (Sec. II), we discuss the partial-locking model in Sec. III and the domain model in Sec. IV. In Sec. V we discuss the experimental situation, concluding that the deviations from perfect locking which are customarily seen do not result in a uniform background, but rather result in distortions of the individual pulse shape. The partial-locking model is shown to be incompatible with experiment, whereas the domain model is in reasonable agreement with it. We also discuss the dynamical basis of the domain model in this section, give some indication of its versatility, and mention remaining problems.

II. GENERAL FORMALISM

In this section we discuss the TPF intensity-correlation experiments which are the subject of this paper, define terms, and introduce the notation and the basic formulas we will use. Consider a material system (usually a dye solution) which is allowed to interact with a narrow band, but otherwise quite arbitrary, optical field $\vec{E}(\vec{r}, t)$ centered at frequency Ω_c. For simplicity, the field is assumed to be linearly polarized, and its transverse variation is neglected, making the problem one dimensional. Usually the field E will be a stochastic process, describable only in terms of an ensemble. We assume further that the matter has a negligible single-photon absorption probability for the field E, but a significant probability for two-photon absorption, followed by fluorescence (TPF).

The field intensity $I(z,t)$ and the two-photon absorption rate $w^{(2)}(z,t)$ can be expressed conveniently in terms of the first- and second-order field correlation functions[12] for the optical field,

$$G^{(1)}(1,2) \equiv \langle E^{(-)}(1) E^{(+)}(2) \rangle \tag{2.1a}$$

and

$$G^{(2)}(1,2,3,4) \equiv \langle E^{(-)}(1) E^{(-)}(2) E^{(+)}(3) E^{(+)}(4) \rangle \ . \tag{2.1b}$$

The arguments of these functions are the space-time points $1 \equiv (z_1, t_1)$, and so forth, and $E^{(\pm)}(1)$ are the positive- and negative-frequency parts of the electric field operator $E(1)$. They annihilate and create a photon at (z_1, t_1), respectively, and satisfy

$$E(1) = E^{(+)}(1) + E^{(-)}(1) \quad \text{with} \quad E^{(-)}(1) = [E^{(+)}(1)]^{\dagger} \ . \tag{2.2}$$

The angular brackets in Eqs. (2.1) denote the quantum expectation value, and also the ensemble average if the field is stochastic, both of which may be represented in a familiar way in terms of the density matrix. In terms of these correlation functions the field intensity at (z_1, t_1) is simply

$$I(1) = G^{(1)}(1,1) ,$$

while under suitable, rather general assumptions,[13] the two-photon absorption rate $w^{(2)}(1)$ is proportional to $G^{(2)}(1,1,1,1)$. We assume that the detector of the subsequent fluorescent emission responds sufficiently slowly that it sees only the integrated fluorescence[14] $\mathfrak{F}(z_1)$ which is given by

$$\mathfrak{F}(z_1) = C \int dt_1 \, G^{(2)}(1,1,1,1) , \tag{2.3}$$

C being a proportionality constant.[15]

For our purposes, the operator nature of E is not important and $E^{(+)}(z, t)$ may be considered equivalent to the analytic signal or complex classical field[16,17] $\mathcal{E}(z,t)$. There is a similar correspondence between $E^{(-)}(z,t)$ and $\mathcal{E}^*(z,t)$. A correlation function can then be expressed as an integral of a product of complex fields weighted by a probability density P. Equations (2.1) assume the form

$$G^{(1)}(1,2) = \int P(\{\epsilon_k\}) \mathcal{E}^*(1) \mathcal{E}(2) \, d^2\{\epsilon_k\}$$

and

$$G^{(2)}(1,2,3,4) = \int P(\{\epsilon_k\}) \mathcal{E}^*(1) \mathcal{E}^*(2) \mathcal{E}(3) \times \mathcal{E}(4) \, d^2\{\epsilon_k\} , \tag{2.4}$$

where $\{\epsilon_k\}$ is the set of complex mode amplitudes defined by the modal decomposition

$$\mathcal{E}(z,t) = \textstyle\sum_k \epsilon_k e^{i(kz - \Omega_k t)} \ . \tag{2.5}$$

Here k is the wave vector of the kth mode and $\Omega_k = v_k k$ is its frequency (v_k is the phase velocity of kth mode). The integral is over the real and imaginary parts of all the mode amplitudes; that is,

$$d^2\{\epsilon_k\} = \Pi_k d(\mathrm{Re}\epsilon_k) \, d(\mathrm{Im}\epsilon_k) \ .$$

In general, the second-order correlation function $G^{(2)}$ is not a simple function of $G^{(1)}$. However, for two important special cases with which we shall be concerned, such a functional relationship does exist. One case is the fully coherent field – for example, the field generated by an idealized noiseless oscillator – in which each mode has a specified complex amplitude ϵ_k' and the probability density for the field is a Dirac δ function,[18]

$$P(\{\epsilon_k\}) = \Pi_k \delta^{(2)}(\epsilon_k - \epsilon_k') \equiv \delta[\mathcal{E}(z,t) - \mathcal{E}'(z,t)]. \quad (2.6)$$

The desired relation between $G^{(2)}$ and $G^{(1)}$,

$$G^{(2)}(1,2,3,4) = G^{(1)}(1,3)G^{(1)}(2,4) + G^{(1)}(1,4)G^{(1)}(2,3), \quad (2.7)$$

results if we substitute Eq. (2.6) into Eqs. (2.4) and perform the integrations.

The particular coherent field with which we are concerned is the field radiated by an ideally mode-locked laser, which consists of a set of modes equally spaced in frequency with adjacent modes separated by a constant phase increment φ. If the radiation originates in a cavity of length L in which the effective velocity is $v = c/n_{\text{eff}}$, the frequency separation is $\Delta\Omega = 2\pi \cdot v/2L$. In the case where the spectrum is uniform, Eq. (2.5) becomes a geometric series which can be summed to yield the familiar repetitive pulsing expression for $\mathcal{E}(z,t)$. Letting m be the number of modes locked, w be the intensity per mode, and Ω_c and φ_c be the frequency and phase of the carrier wave, the expression is[19]

$$\mathcal{E}(z,t) = w^{1/2} e^{-i\theta_c} (\sin \tfrac{1}{2} m\theta)/(\sin \tfrac{1}{2}\theta), \quad (2.8)$$

where
$$\theta_c \equiv \Omega_c(t + z/v) + \varphi_c$$
and
$$\theta \equiv \Delta\Omega(t + z/v) + \varphi. \quad (2.9)$$

The corresponding intensity is

$$I(z,t) = |\mathcal{E}(z,t)|^2, \quad (2.10)$$

and the average intensity, obtained by integrating Eq. (2.10) over the period of the pulse train or the cavity round-trip time $2L/v = 2\pi/\Delta\Omega$ is

$$W = \frac{\Delta\Omega}{2\pi} \int_0^{2\pi/\Delta\Omega} dt\, I = mw. \quad (2.11)$$

From Eq. (2.10) it also follows that the peak intensity is $mW = m^2 w$ and the pulse half-width is $2\pi/m\Delta\Omega$ to the first zero.

The second important case in which there exists a simple relation between $G^{(2)}$ and $G^{(1)}$ is that of a thermal field obeying Gaussian statistics. In this case the real and imaginary parts of all ϵ_k are uncorrelated Gaussian variates, so that the field probability density is

$$P(\{\epsilon_k\}) = \prod_k \frac{1}{2\pi\sigma_k^2} \exp\left(-\frac{|\epsilon_k|^2}{2\sigma_k^2}\right), \quad (2.12)$$

where $\sigma_k^2 = \langle (\text{Re}\epsilon_k)^2 \rangle = \langle (\text{Im}\epsilon_k)^2 \rangle$.

Substituting Eq. (2.12) into Eqs. (2.4) yields the desired expression[12] for $G^{(2)}$,

$$G^{(2)}(1,2,3,4) = G^{(1)}(1,3)G^{(1)}(2,4) + G^{(1)}(1,4)G^{(1)}(2,3). \quad (2.13)$$

The importance of the Gaussian field is a result of the central-limit theorem of statistics, whereby the sum of a sufficiently large number of independent random variables asymptotically obeys Gaussian statistics. Our interest in it is to describe the output of an unlocked multimode solid-state laser, the modes of which in crudest approximation have fixed amplitudes, but independent, uniformly distributed random phases. Since the number of modes m is typically large (from many hundreds to tens of thousands), the conditions for the central-limit theorem to apply are met and the total field E is approximately Gaussian. It can be shown[20] that the relative error in this approximation is of order m^{-1} and, hence, is very small for a reasonably large number of modes.[21]

Two common configurations for TPF experiments are shown in Fig. 1. In Fig. 1(a) the beam from the source laser L is divided by a 50% beam splitter M, the two beams then passing in opposite directions through the dye cell C. The point of equal-path difference is labeled $z = 0$, and the positive z direction is indicated by an arrow. In Fig. 1(b) the radiation from the source passes through the dye cell in the negative direction and is reflected back upon itself by a 100% mirror M' at $z = 0$. In either case, the fluorescence is monitored from the side by photographic means or in rare cases photoelectric means.

With mirror M' absent, only the wave traveling

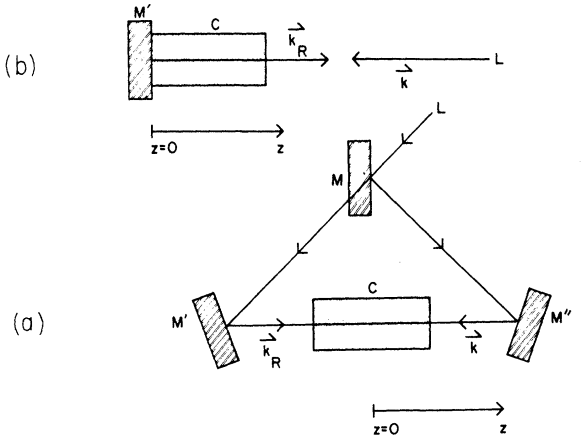

FIG. 1. Two common configurations for TPF experiments (C is the dye cell; M', M'' are 100% mirrors; M is a 50% mirror; L is the source laser; $\vec{k}$ and $\vec{k}_R$ are wave vectors of colliding beams).

in the $-z$ direction remains in the liquid; we denote it by $E(z,t)$. Also, we denote the wave traveling in the $+z$ direction by $E_R(z,t)$. Clearly,

$$E_R(z,t) = -E(z,t-\tau)\ , \tag{2.14}$$

where $\tau \equiv 2nz/c$ is the relative delay between the two beams. (Here n is the refractive index of the dye solution.) The minus sign occurs in Eq. (2.14) because E has undergone an even number of reflections, while E_R has undergone an odd number. The total field is then given by $E(z,t)+E_R(z,t)$.

If one substitutes the total field $E+E_R$ for E in Eq. (2.1b), 16 terms ensue. The expression for the fluorescence obtained by using this sum for $G^{(2)}$ in Eq. (2.3) appears to be rather complicated. However, it simplifies considerably in the usual case where the spatial resolution limit of the detector is greater than the optical wavelength.[4] Denoting the spatial average of the fluorescence $\mathfrak{F}$ over a wavelength by F, we have[22]

$$F(\tau) = C\int dt[\langle E^{(-)2}E^{(+)2}\rangle + \langle E_R^{(-)2}E_R^{(+)2}\rangle + 4\langle E^{(-)}E_R^{(-)}E_R^{(+)}E^{(+)}\rangle], \tag{2.15}$$

where the spatial argument z has been replaced by the time difference τ, to which it is proportional.

It is useful to normalize the fluorescence by referring it to the fluorescence $F_0(\tau)$ produced by a single pass of the optical beam,[23] which can be measured easily by removing mirror M' in Fig. 1. Setting $E_R \equiv 0$ in Eq. (2.15), we obtain

$$F_0(\tau) = C\int dt\,\langle E^{(-)2}E^{(+)2}\rangle\ . \tag{2.16}$$

So far we have neglected to mention the limits of the time integrations in the expressions for the fluorescence. Since the radiation originates in a cavity of length L, the radiation has a discrete spectrum of modes separated at least approximately[24] in frequency by $\Delta\Omega = 2\pi\cdot v/2L$, and its amplitude will be nearly periodic with period $2\pi/\Delta\Omega$. Thus it seems natural to choose one or more full periods as the range of the time integrals. Then $F(\tau)$ will be approximately periodic in z with period L, and $F_0(\tau)$, the single-pass reference fluorescence of Eq. (2.16), will be nearly independent of z on a macroscopic scale.

If, as is generally true, the quasiperiod $2\pi/\Delta\Omega$ of the emission is much greater than the inverse bandwidth of its intensity fluctuations, the TPF pattern consists of regions of enhanced fluorescence superimposed on a uniform background. The regions of enhancement have maxima at $\tau = 2\pi j/\Delta\Omega$ $(j = 0, \pm1, \pm2, \ldots)$ and widths of the order of the inverse bandwidth. Focusing our attention on the region near $\tau = 0$, we denote the peak fluorescence by $F_p \equiv F(0)$ and the background fluorescence by F_b. Now a parameter widely used to characterize the emission is the peak-to-background contrast ratio

$$R \equiv F_p/F_b\ . \tag{2.17}$$

However, with little additional effort for the experimenter or the theorist, it is possible to obtain two parameters, from which one can characterize the field more fully than is possible simply from the value of R. These parameters are obtained by referring the fluorescence F to the single-pass fluorescence F_0, enabling us to define a peak-to-reference contrast ratio

$$R_p \equiv F_p/F_0 \tag{2.18}$$

and a background-to-reference contrast ratio

$$R_b \equiv F_b/F_0\ . \tag{2.19}$$

We conclude this section with a clarifying remark. The objection might be raised that we should not take an ensemble average of the field products even if the field is random, since the experiment described involves only a single firing of the laser. The response to this objection is that there are many stochastic influences within the laser causing the random parameters to evolve in time through values corresponding to several members of the ensemble. If the observation time in the experiment is sufficiently long, we could, in effect, be performing an ensemble average.[6] Whether we are or not is a question for experiment or a more detailed theory to answer.

This completes our discussion of the general formalism. In Secs. III and IV we use these results in discussing two different models for imperfectly locked lasers.

III. PARTIAL-LOCKING MODEL

In this section we investigate the TPF for a model of a partially mode-locked laser, in which a portion of the modes near the center of the line are locked and the rest are unlocked, with random phases relative to one another. This model bridges the gap, in a rather natural way, between the extremes of perfectly locked and completely unlocked operation. Conceivably, it could describe the emission from an actual laser in which the parametric effects responsible for mode locking are sufficiently high to lock some, but not all, of the oscillating modes.[25]

Assume that there are m oscillating modes, m_l of which are locked and m_u unlocked. Thus

$$m = m_l + m_u\ . \tag{3.1}$$

We wish to develop analytic means of treating the TPF problem. Of course, an exact solution is not possible. However, we will make use of the fact that typical oscillating solid-state lasers sup-

port a large number of modes to obtain useful approximate results. To achieve this goal, we begin by splitting each of the fields E and E_R into parts corresponding to locked and to unlocked modes,

$$E^{(\pm)} = E_l^{(\pm)} + E_u^{(\pm)} \quad \text{and} \quad E_R^{(\pm)} = E_{Rl}^{(\pm)} + E_{Ru}^{(\pm)} \ . \tag{3.2}$$

As discussed in Sec. II, if m_u is sufficiently large, E_u and E_{Ru} obey Gaussian statistics.

The fluorescence for this model is obtained by substituting Eqs. (3.2) into Eq. (2.15). The resulting expression contains 48 terms. To simplify it, first we observe that E_l and E_u are uncorrelated, so that averages of their products reduce to products of averages; for example,

$$\langle E_u^{(-)} E_l^{(-)} E_u^{(+)2} \rangle = \langle E_l \rangle \langle E_u^{(-)} E_u^{(+)2} \rangle \ .$$

Secondly, we note that averages of products of $E_u^{(\pm)}$ containing unequal numbers of positive- and negative-frequency fields vanish, due to the stationarity of the Gaussian distribution, Eq. (2.12); for example,

$$\langle E_u^{(-)} E_u^{(+)2} \rangle = 0.$$

With these simplifications the fluorescence is given by

$$\begin{aligned} F(\tau) = C \int dt \{ & \langle E_l^{(-)2} E_l^{(+)2} \rangle + \langle E_{Rl}^{(-)2} E_{Rl}^{(+)2} \rangle \\ & + 4 \langle E_l^{(-)} E_{Rl}^{(-)} E_{Rl}^{(+)} E_l^{(+)} \rangle + \langle E_u^{(-)2} E_u^{(+)2} \rangle \\ & + \langle E_{Ru}^{(-)2} E_{Ru}^{(+)2} \rangle + 4 \langle E_u^{(-)} E_{Ru}^{(-)} E_{Ru}^{(+)} E_u^{(+)} \rangle \\ & + 4 [\langle E_l^{(-)} E_l^{(+)} \rangle \langle E_u^{(-)} E_u^{(+)} \rangle \\ & + \langle E_{Rl}^{(-)} E_{Rl}^{(+)} \rangle \langle E_{Ru}^{(-)} E_{Ru}^{(+)} \rangle \\ & + \langle E_l^{(-)} E_l^{(+)} \rangle \langle E_{Ru}^{(-)} E_{Ru}^{(+)} \rangle \\ & + \langle E_{Rl}^{(-)} E_{Rl}^{(+)} \rangle \langle E_u^{(-)} E_u^{(+)} \rangle \\ & + \langle E_l^{(-)} E_{Rl}^{(+)} \rangle \langle E_{Ru}^{(-)} E_u^{(+)} \rangle \\ & + \langle E_{Rl}^{(-)} E_l^{(+)} \rangle \langle E_u^{(-)} E_{Ru}^{(+)} \rangle] \} \ . \end{aligned} \tag{3.3}$$

The first six terms of this expression can be simplified further by using the properties of coherent and of Gaussian fields given by Eqs. (2.7) and (2.13). Defining

$$I_l \equiv \langle E_l^{(-)} E_l^{(+)} \rangle \ , \quad I_{Rl} \equiv \langle E_{Rl}^{(-)} E_{Rl}^{(+)} \rangle \ , \quad I_u \equiv \langle E_u^{(-)} E_u^{(+)} \rangle \ , \quad I_{Ru} \equiv \langle E_{Ru}^{(-)} E_{Ru}^{(+)} \rangle \ , \tag{3.4}$$

$$G_l \equiv \langle E_l^{(-)} E_{Rl}^{(+)} \rangle \quad \text{and} \quad G_u \equiv E_u^{(-)} E_{Ru}^{(+)} \rangle \ , \tag{3.5}$$

Eq. (3.3) takes the form[9]

$$\begin{aligned} F(\tau) = C \int dt \{ & I_l^2 + I_{Rl}^2 + 4 I_l I_{Rl} \\ & + 2 I_u^2 + 2 I_{Ru}^2 + 4 I_u I_{Ru} + 4 |G_u|^2 \\ & + 4 [I_l I_u + I_{Rl} I_{Ru} + I_l I_{Ru} + I_{Rl} I_u + G_l G_u^* + G_l^* G_u] \} \ . \end{aligned} \tag{3.6}$$

Here I denotes the intensity of that portion of the field designated by the appended subscripts, and G denotes the cross-correlation function between the oppositely directed waves.

From Eq. (3.6) one easily obtains the peak, background, and reference fluorescence. At $\tau = 0$, we have $I_l = I_{Rl} = -G_l = -G_l^*$ and $I_u = I_{Ru} = -G_u = -G_u^*$, so that the peak fluorescence is

$$F_p = 6C \int dt \, (I_l^2 + 2 I_u^2 + 4 I_l I_u) \ . \tag{3.7}$$

On the other hand, when τ is much greater than the inverse bandwidths of both the locked and unlocked portions of the field (that is, the coherence time of E_u and the pulse width of E_l), one has $G_u = G_u^* = 0$ and $G_l = G_l^* = 0$. If, in addition, one uses the general results for arbitrary τ,

$$I_u = I_{Ru} \quad \text{and} \quad \int_0^{2\pi/\Delta\Omega} dt \, I_l^2 = \int_0^{2\pi/\Delta\Omega} dt \, I_{Rl}^2 \ ,$$

the background fluorescence is found to be

$$F_b = 2C \int dt \, (I_l^2 + 4 I_u^2 + 8 I_l I_u) \ . \tag{3.8}$$

Finally, by setting $E_R \equiv 0$, the reference fluorescence becomes

$$F_0 = F_{0l} + F_{0u} + F_{0,\mathrm{int}} \ , \tag{3.9}$$

where F_{0l}, F_{0u}, and $F_{0,\mathrm{int}}$ are the reference fluorescence due to the locked modes alone, due to the unlocked modes alone, and due to their interaction, respectively, defined by

$$F_{0l} = C \int dt \, I_l^2 \ , \tag{3.10a}$$

$$F_{0u} = C \int dt \, I_u^2 \ , \tag{3.10b}$$

$$\text{and} \quad F_{0,\mathrm{int}} = 4C \int dt \, I_l I_u \ . \tag{3.10c}$$

Using Eqs. (2.17)–(2.19) and (3.7)–(3.10), the peak-to-single-pass and background-to-single-pass contrast ratios are then

$$R_p = 6 \tag{3.11a}$$

$$\text{and} \quad R_b = 4 - 2F_{0l}/F_0 \ , \tag{3.11b}$$

and the peak-to-background contrast ratio is [9]

$$R = 3(2 - F_{0l}/F_0)^{-1} \ . \tag{3.12}$$

At this point we must make some assumption concerning the spectrum of the field. For simplicity we assume that the spectrum is uniform, and call the intensity per mode w. Then the complex amplitude $\mathcal{E}_l(z,t)$, the instantaneous intensity $I_l(z,t)$, and the average intensity W_l for the locked portion of the field are given by Eqs. (2.8)–(2.11). Substituting Eqs. (2.10) and (2.8) into Eq. (3.10a) yields a value for F_{0l},

$$F_{0l} = \frac{2Cw^2}{\Delta\Omega} \int_0^{\pi} dx \frac{\sin^4 m_l x}{\sin^4 x} \ .$$

The integral in this expression can be evaluated

exactly,[26] yielding $\frac{1}{3}\pi m_l(2m_l^2+1)$, so that

$$F_{0l}=\tfrac{4}{3}\pi C\Delta\Omega^{-1}w^2m_l(m_l^2+\tfrac{1}{2}) \quad . \tag{3.13}$$

Since the mean intensity of the unlocked portion of the field is $W_u=m_uw=I_u$, we have the further results that

$$F_{0u}=4\pi C\Delta\Omega^{-1}w^2m_u^2 \tag{3.14}$$

and, using Eq. (2.11),

$$F_{0,\mathrm{int}}=8\pi C\Delta\Omega^{-1}w^2m_lm_u \quad . \tag{3.15}$$

Using Eqs. (3.13)–(3.15) and Eq. (3.9), the contrast ratio R of Eq. (3.12) becomes

$$R=3(1+\zeta_l/m)/(1+2\zeta_l/m) \quad , \tag{3.16}$$

where $$\zeta_l\equiv 3(1-\eta_l^2)\eta_l^{-3}[2m_l^2/(2m_l^2+1)] \tag{3.17}$$

and $\eta_l\equiv m_l/m$ is the fractional number of modes locked. Note that ζ_l can be considered, for all practical purposes, to be a function only of η_l and not of m, since the factor in brackets is always nearly unity.

In Fig. 2 the contrast ratio R given by Eq. (3.16) is plotted versus η_l over the range 100–4% for various values of m. Assuming that the mode spacing is $\Delta\Omega=2\pi\times10^8$ sec^{-1}, corresponding to the longitudinal mode spacing in a 150-cm cavity, the values chosen for m correspond to several realistic choices for the spectral width $\delta\lambda$. The values of m and $\delta\lambda$ and their realizations are: (i) $m=53\,200$, $\delta\lambda=200$ Å (fluorescent linewidth of 1.06-μ Nd-glass laser); (ii) $m=26\,600$, $\delta\lambda=100$ Å (oscillating width of mode-locked Nd-glass laser emission[1]); (iii) $m=3100$, $\delta\lambda=5$ Å (oscillating width of mode-locked 6943 Å-ruby-laser emission[27]); and (iv) $m=532$, $\delta\lambda=2$ Å (Nd^{3+}: YAG laser linewidth). In addition, the curve for $m=100$ is plotted for comparison with an existing computer calculation.[8]

On the basis of Eqs. (3.12) and (3.16), Fig. 2, and the preceding discussion, we can summarize

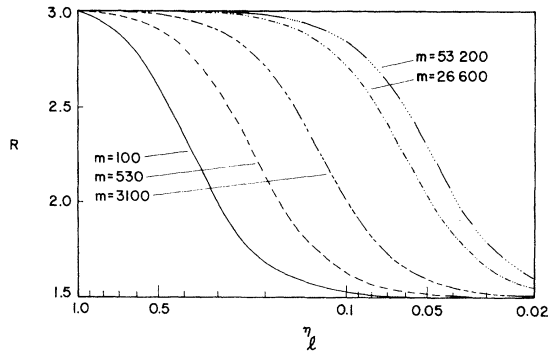

FIG. 2. TPF peak-to-background contrast ratio R in the partial-locking model as a function of the fraction η_l of modes which are locked for various realistic values of the total number of modes m.

the properties of the fluorescence in this model.

(a) The results reduce to the usual results for perfect locking and for no locking when we set $\eta_l=1$ ($F_{0l}=F_0$) and $\eta_l=0$ ($F_{0l}=0$), respectively. For $\eta_l=1$, the peak-to-single-pass, background-to-single-pass, and peak-to-background contrast ratios are $R_p=6$, $R_b=2$, and $R=3$, respectively. The value $R_b=2$ reflects the lack of overlap between the oppositely directed waves in the background region. On the other hand, for $\eta_l=0$ we have $R_p=6$, $R_b=4$, and $R=1.5$.

(b) In the general case, the value of R varies monotonically between the values of 3 and 1.5, found for the two limiting cases. However, the normalized peak fluorescence R_p does not change as η_l is increased from 0 to 1, the lowering of R being due instead to an increase of the normalized background fluorescence R_b. The reason for this behavior is clear: R_p does not decrease because the noise is still coherent with itself over very short times; on the other hand, R_b increases above twice the single-pass value because the oppositely directed waves now overlap and there will be a cross term in the two-photon absorption corresponding to the absorption of one photon from each beam.

(c) The various contrast ratios are all independent of the intensity per mode w and of the mode spacing $\Delta\Omega$.

(d) The contrast ratio R depends strongly on the total number of modes m and not only the fraction η_l which are locked. As m increases, R falls off more slowly with decreasing η_l (increasing percentage of modes unlocked). The reason for this is that the importance of the fluorescence from the locked modes relative to that from the unlocked modes increases when the mode number is increased. For example, if m is doubled while keeping η_l and the average intensity mw constant, it follows from Eqs. (3.13) and (3.14) that the fluorescence from the locked modes over a given time interval will double, while the fluorescence from the unlocked modes will remain the same. This is true whether we increase m by increasing the total bandwidth while keeping the mode spacing $\Delta\Omega$ fixed or by decreasing the mode spacing while keeping the bandwidth $m\Delta\Omega$ constant. In passing we note that, if some spectral shape other than a uniform one is assumed, the importance of the locked modes will be enhanced further since they occupy the central portion of the line.

(e) The half-width at half-maximum of a peak of the fluorescence trace is proportional to the pulse half-width Δt (also at half-maximum). In terms of the variable τ, the proportionality factor is of order unity, its actual value depending on

the pulse shape. For our case, in which the pulse shape is given by Eqs. (3.16) and (3.17), we have [28] $\Delta t = 0.88\pi/m_l\Delta\Omega$, and the proportionality factor is about 1.5.

Since the assumption that the sum of the unlocked-mode amplitudes is a Gaussian variate is in error by terms of relative magnitude m_u^{-1}, one would tend to lose confidence in this approximation for very small m_u (say $m_u <\sim 10$). This region is not important unless the total number of modes m is small. In that case it becomes necessary to resort to computer calculations of the TPF.[8] Since the computer calculation is unfeasible for large mode numbers, the amount of time required varying approximately as m^3, it is clear that the computer solutions and the above approximate analytic solutions complement one another.

We now consider briefly another aspect of this model, namely, the single-photon photodetection problem. The peak intensity of the mode-locked field E_l is

$$I_p = m_l W_l = m_l^2 w \ ,$$

and the background intensity due to the noise is

$$I_b = W_u = m_u w \ .$$

The peak-to-background "contrast" in the intensity $I(t)$ is given by

$$I_p/I_b = m\eta_l^2/(1-\eta_l) \ .$$

This ratio is proportional to m, so that the peak intensity will dominate the noisy background increasingly as m gets larger.

If one had a fast photodiode-oscilloscope combination with a response time T_d less than the width $\Delta t = (m_l\Delta\Omega/2\pi)^{-1}$ of the mode-locked pulses, one would see peaks with the above contrast in the oscilloscope trace. However, since T_d is limited to about 0.1 nsec, the photocurrent $\mathcal{I}(t)$ will have a contrast determined by the total energy in the pulse rather than its peak power, resulting in a marked reduction in the prominence of the pulse. To see this, assume that the detector impulse response $g(t)$ is exponential

$$g(t) = T_d^{-1} e^{-t/T_d} , \quad (t \geq 0)$$
$$= 0, \quad (t < 0) \ .$$

Then, for the pulse width $\Delta t \ll T_d$, the peak photocurrent is related to the peak intensity by[29] $\mathcal{I}_p = (\alpha\Delta t/T_d)I_p$, where α is the quantum efficiency of the detector, while the background variables are related by $\mathcal{I}_b = \alpha I_b$. The contrast r of the oscilloscope trace will be

$$r \equiv \mathcal{I}_p/\mathcal{I}_b = (2\pi/\Delta\Omega T_d)[\eta_l/(1-\eta_l)] \ . \qquad (3.18)$$

As expected, this result is independent of m, but depends on a parameter $\beta \equiv 2\pi/\Delta\Omega T_d$.

In Fig. 3 the contrast r in the photocurrent trace is plotted as a function of η_l for several values of the parameter β. It is seen that β is the ratio of the time between pulses $t_{\text{pulse}} = 2\pi/\Delta\Omega$ to the detector response time. It has been tacitly assumed above that the detector is fast enough so that $T_d < t_{\text{pulse}}$; consequently, we require $\beta > 1$.

It is interesting to contrast the behavior of the (time-resolved) photocurrent from a fairly fast detector with that of the (integrated) TPF. The contrast r in the former case does not change if one merely increases the number of modes, keeping η_l and $\Delta\Omega$ constant,[30] whereas the contrast ratio R in the latter case increases with increasing m. The difference in behavior can be attributed to the fact that although both $\mathcal{I}(t)$ and $F(\tau)$ are given by time integrals of functions of the intensity, the first integral is linear in the intensity and the second is nonlinear.

By combining Eqs. (3.16) and (3.18), the TPF contrast ratio R can be plotted versus the photocurrent contrast r. This is done in Fig. 4. The function forms a two-parameter family of curves. The results are plotted for various values of the parameter m and only one value of the parameter β, namely, $\beta = 40$, which corresponds, for example, to a time between pulses $t_{\text{pulse}} = 10^{-8}$ sec and a detector response time $T_d = 2.5\times10^{-10}$ sec. It is clear from the figure that, for any reasonable mode number, a large background must appear on the oscilloscope before the contrast ratio will differ significantly from Fig. 3.

This completes our discussion of the partial-locking model. In Sec. IV we discuss the domain model.

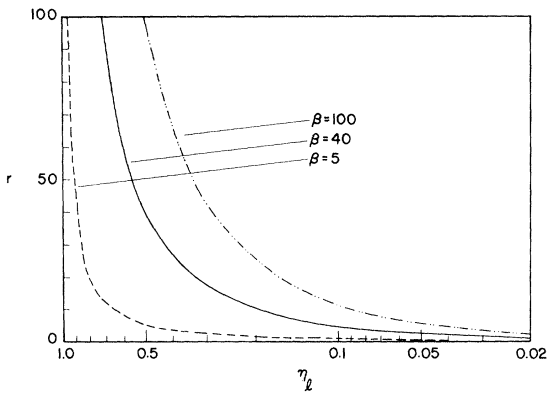

FIG. 3. Ratio r of the peak to the background photocurrent in the partial-locking model as a function of the fractional number of modes locked η_l for various values of β. The parameter β is the ratio of the pulse separation to the detector resolution time T_d. It is assumed that the pulse length is much smaller than T_d.

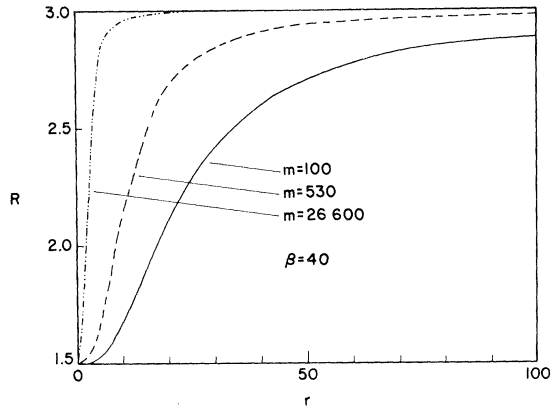

FIG. 4. TPF contrast ratio R as a function of the photocurrent "contrast" r in the partial-locking model. The function is plotted for several values of the number of modes m, and one value of the parameter β (defined as in Fig. 3).

IV. DOMAIN MODEL

In this section we present a simple alternative model for the emission from mode-locked lasers. We call it the "domain model" because of a loose analogy with the case of ferromagnetism. Here the "domains" are regions in frequency space; the oscillating spectrum consists of groups of adjacent modes, or domains, with perfect locking of the modes within each group. The intermode spacing is constant within a group, but varies from one group to another, and the spectral widths of the groups need not coincide. Each group constitutes a pulse train, consisting of an amplitude-modulated carrier wave, whose duration is the inverse spectral width of the group. We take the phases of the carrier waves to be uniform random variables and require that the peaks of the pulses corresponding to each group coincide approximately in time. Then, although the total field will still be a train of pulses whose widths are approximately the inverse of the width of a single group, the various group amplitudes will interfere, giving rise to fluctuations within the pulse envelope, whose coherence time is the inverse of the total spectral width. If the number of groups is reasonably large, by the central-limit theorem, the resulting field will closely resemble a train of band-limited-noise pulses (that is, white light passed through a filter and a chopper), from which one can readily infer the gross features of the resulting TPF traces.

Following these qualitative remarks, we would like to express quantitatively the behavior of the field intensity. Assume that there are $M=2N+1$ domains, the ith one containing m_i modes and having amplitude $E_i \equiv E_i(z,t)$. The total number of modes is then

$$m=\sum_{i=1}^{M} m_i \ ,$$

and the total field is

$$E^{(\pm)}(z,t)=\sum_{i=1}^{M} E_i^{(\pm)}(z,t) \ . \tag{4.1}$$

From Eq. (4.1) the field intensity is simply

$$I(z,t)\equiv G^{(1)}(z,t;\,z,t)=\textstyle\sum_i \sum_j \langle E_i^{(-)} E_j^{(+)}\rangle \ . \tag{4.2}$$

Since every E_i is a fully coherent field, we may write

$$\langle E_i^{(-)} E_j^{(+)}\rangle = \mathcal{E}_i^* \mathcal{E}_j \ , \tag{4.3}$$

where, by analogy with Eqs. (2.8)–(2.9),

$$\mathcal{E}_i(z,t)=w_i^{1/2} e^{-\theta_{ci}} (\sin \tfrac{1}{2} m_i \theta_i)/(\sin \tfrac{1}{2}\theta_i). \tag{4.4}$$

In the latter equation

$$\theta_{ci} \equiv \Omega_{ci}(t+z/v_i)+\varphi_{ci} \tag{4.5a}$$

and

$$\theta_i \equiv \Delta\Omega_i (t+z/v_i)+\varphi_i \ , \tag{4.5b}$$

where Ω_{ci} is the carrier frequency of the ith group and φ_{ci} is its random phase, v_i is the velocity of the ith group, and $\Delta\Omega_i = 2\pi \cdot v_i/2L$ is the corresponding mode separation. The phase φ_i determines the location of the peak of $\mathcal{E}_i$. Although we only need require the spread in φ_i to be less than $2\pi/m_i$ to obtain a single pulse per cavity round-trip time, we assume for simplicity that $\varphi_i = \varphi$ independent of i in what follows. Note that, in writing Eq. (4.4), we have assumed that each mode of the ith group has the same amplitude, but have allowed for the possibility of the amplitude varying from one group to another, w_i being the intensity per mode within the ith group. With the help of Eqs. (4.3) and (4.4), Eq. (4.2) becomes

$$\begin{aligned} I(z,t)=&\sum_{i}^{M} w_i[\sin^2(\tfrac{1}{2}m_i\theta_i)/\sin^2(\tfrac{1}{2}\theta_i)] \\ &+\sum_{i,j}^{M}{}' (w_i w_j)^{1/2}\cos(\theta_{ci}-\theta_{cj}) \\ &\times[\sin(\tfrac{1}{2}m_i\theta_i)/\sin(\tfrac{1}{2}\theta_i)] \\ &\times[\sin(\tfrac{1}{2}m_j\theta_j)/\sin(\tfrac{1}{2}\theta_j)] \ . \end{aligned} \tag{4.6}$$

The prime on the sum indicates that the terms for which $i=j$ are omitted.

In Fig. 5 the intensity of Eq. (4.6) is plotted versus t with z fixed over an interval corresponding to the central lobe of a single pulse. The summations were performed on a computer, and the results are shown for two different choices of the set of random phases $\{\varphi_{ci}\}$. The parameters chosen are appropriate for mode-locking of a Q-switched Nd-glass laser in a 150-

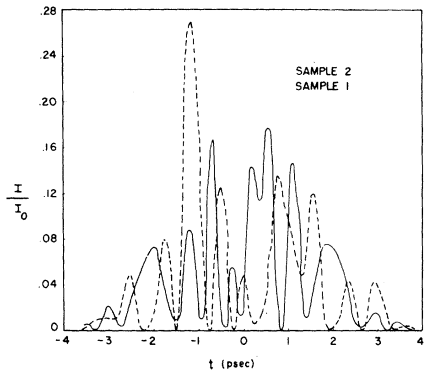

FIG. 5. Relative intensity I/I_0 as a function of time t in the domain model for two sample functions corresponding to different choices of the set of relative phases φ_{ci} between the groups of modes, showing random substructure within a pulse. The normalizing factor I_0 is the peak intensity in the corresponding perfectly locked case. The field consists of 26 600 modes equal in intensity, 11 groups of equal size.

cm cavity. The spectral width is $\delta\lambda = 100$ Å and the mode spacing is $\Delta\Omega_i = \Delta\Omega = 2\pi \times 10^8\ \mathrm{sec}^{-1}$. It is assumed that the modes (total number $m = 26\,600$) form 11 groups ($M = 11$, $N = 5$), each containing an equal number of modes $m_i \cong 26\,600/11$, and that the spectrum is uniform. The value of φ is chosen such that the pulse is centered near $t = 0$, and the intensity is normalized by dividing it by the peak intensity $I_0 = (\sum_i w_i^{\frac{1}{2}} m_i)^2$, in the corresponding perfectly locked case (obtained by setting $\varphi_{ci} = 0$ for $i = 1, \ldots, M$). By performing a crude Monte Carlo calculation, considering $\{\varphi_{ci}\}$ to be random variates, we obtain an estimate for the expectation value of the pulse shape. The results of such a calculation are shown in Fig. 6, which represents the average of the intensities of 60 sample pulses. Figure 6 shows that the average is approaching the shape of the pulse corresponding to a single mode group, as expected from Eq. (4.6). Some residual fluctuations remain due to the poor convergence. The pulse half-width is 1.75 psec, which is consistent[28] with the inverse spectral width of a single group of modes (4.14 psec). From Fig. 5 the individual samples appear to have substantial substructure on a scale of the inverse spectral width (0.376 psec). The results of Figs. 5 and 6 are to be compared with Fig. 7(a), which shows the intensity for the corresponding perfectly locked field.

Before leaving our discussion of the field intensity in the domain model, let us consider briefly the results of a photodetection experiment with a fast detector. Using the notation of Sec. III, it is clear that $\mathcal{I}(t)$ consists of a sequence of pulses, whose shape is characteristic of the impulse response of the detection system. Thus the contrast r is infinite, as in the perfect-locking case.

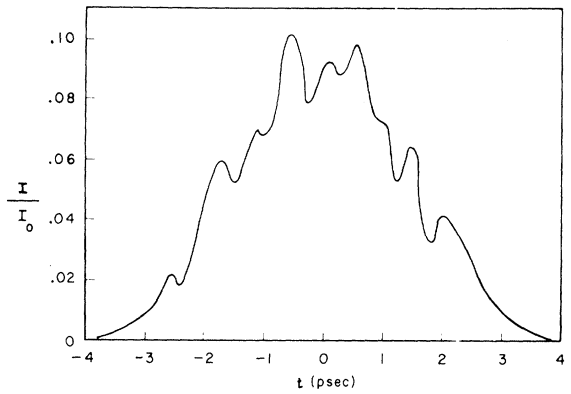

FIG. 6. Relative intensity $I(t)/I_0$ for the average of 60 pulses corresponding to different sets of phases φ_{ci}.

We now consider the TPF in the domain model. The reflected field can be written as a sum over the amplitudes of the individual groups,

$$E_R^{(\pm)}(z, t-\tau) = \sum_i E_{Ri}^{(\pm)}, \tag{4.7}$$

where $E_{Ri}^{(\pm)} \equiv -E_i^{(\pm)}(z, t-\tau)$. Substitution of Eqs. (4.1) and (4.7) into Eq. (2.15) leads one to an expression for $F(\tau)$ involving three fourfold sums over the group indices. However, the sums reduce to twofold and single summations, because each of the groups has a different center frequency Ω_i with the result that the time integrals, such as

$$f_{ijkl}^{(1)}(\tau) \equiv \int dt \langle E_i^{(-)} E_{Rj}^{(-)} E_{Rk}^{(+)} E_l^{(+)} \rangle\ ,$$

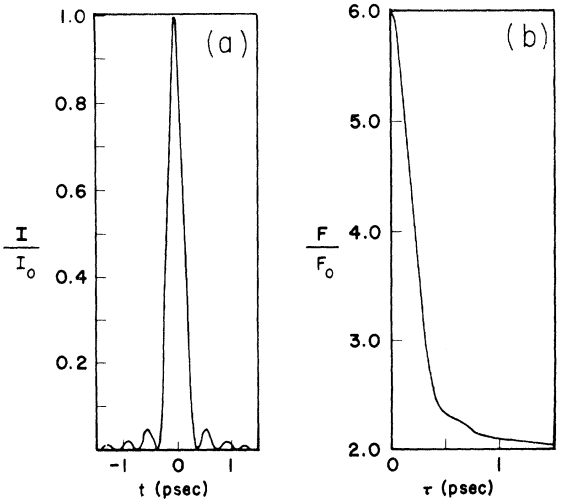

FIG. 7. (a) Relative intensity $I(t)/I_0$ for the perfectly locked case corresponding to Fig. 5; (b) the corresponding TPF yield F, referred to the single-pass fluorescence F_0, as a function of the time delay τ.

for example, will be small unless $\Omega_i+\Omega_j-\Omega_k-\Omega_l=0$. We also note that each of the fields E_i is fully coherent, so that, for example,

$$\langle E_i^{(-)}E_{Rj}^{(-)}E_{Rk}^{(+)}E_l^{(+)}\rangle = \mathcal{E}_i^*\mathcal{E}_{Rj}^*\mathcal{E}_{Rk}\mathcal{E}_l ,$$

where $\mathcal{E}_{Rk}\equiv-\mathcal{E}_k(z,t-\tau)$. Thus

$$f_{ijkl}^{(1)}(\tau)=\int dt\,[\,|\mathcal{E}_i|^2|\mathcal{E}_{Rj}|^2\delta_{il}\delta_{jk}(1-\delta_{ij}) + \mathcal{E}_i^*\mathcal{E}_{Rj}^*\mathcal{E}_{Ri}\mathcal{E}_j\delta_{ik}\delta_{jl}(1-\delta_{ij}) + |\mathcal{E}_i|^2|\mathcal{E}_{Ri}|^2\delta_{ij}\delta_{ik}\delta_{il}\,] ,$$

with similar results for the other integrals in Eq. (2.15). The resulting fluorescence is

$$F(\tau)=C\int dt'\,[\textstyle\sum_i (I_i^2+I_{Ri}^2+4I_iI_{Ri}) + 2\sum_{i,j}(I_iI_j+I_{Ri}I_{Rj}+2I_iI_{Rj}+2G_iG_j^*)] , \qquad (4.8)$$

where $I_i\equiv\langle E_i^{(-)}E_i^{(+)}\rangle=|\mathcal{E}_i|^2$,

$$I_{Ri}\equiv\langle E_{Ri}^{(-)}E_{Ri}^{(+)}\rangle=|\mathcal{E}_{Ri}|^2 , \qquad (4.9)$$

and $G_i\equiv\langle E_i^{(-)}E_{Ri}^{(+)}\rangle=\mathcal{E}_i^*\mathcal{E}_{Ri}$.

In contrast to the partially locked case the peak and background fluorescence can both be expressed simply in terms of the single-pass fluorescence F_0. To obtain F_0 we set E_R equal to zero, with the result

$$F_0=C\int dt\,(\textstyle\sum_i I_i^2+2\sum_{i,j}' I_iI_j) . \qquad (4.10)$$

At $\tau=0$, we have

$$I_i=I_{Ri}=-G_i=-G_i^*\,(i=1,\ldots,M);$$

consequently, according to Eq. (4.8), the peak fluorescence is

$$F_p=6F_0 , \qquad (4.11a)$$

so that $R_p=6$. (4.11b)

When τ is greater than the inverse bandwidth of the smallest group of modes, either I_i or I_{Rj} is zero for any value of t and, moreover, $G_i=G_i^*=0$. Consequently, the last term of the single sum in Eq. (4.8) and the last two terms of the double sum do not contribute to the background fluorescence F_b. If we make use of the relation

$$\int_0^{2\pi/\Delta\Omega} dt\,I_iI_j=\int_0^{2\pi/\Delta\Omega} dt\,I_{Ri}I_{Rj} ,$$

the result is

$$F_b=2F0 \qquad (4.12a)$$

or $R_b=2$. (4.12b)

Combining this result with Eq. (4.11), we have

$$R\equiv F_p/F_b=3 . \qquad (4.13)$$

Neither Eq. (4.11) nor (4.12) is surprising, both results agreeing with those for the perfectly locked case. The total field has a high degree of temporal coherence for short delays, so that $R_p=6$. Moreover, since the field is a pulse train, there are regions in the fluorescence cell where there is no overlap between the oppositely directed waves, so that the fluorescence is just twice that from a single pass. Nevertheless, a striking difference from the perfectly locked case arises if we consider in more detail how $F(\tau)$ varies between the peak and background regions. The terms involving I_i have widths at least $\sim 2\pi/m_i\Delta\Omega_i$, the inverse bandwidth of a single domain, whereas the sum involving G_i has a much narrower width. We show that this sum, denoted by

$$S(\tau)\equiv\sum_{i,j}{}'G_iG_j^* , \qquad (4.14)$$

vanishes approximately when $\tau>\sim 2\pi/\sum_i m_i\Delta\Omega_i$, the inverse of the total bandwidth. It follows that there is a middle range of values of τ for which all the terms of Eq. (4.8) except the last are important. The fluorescence in this middle region is

$$F_m=C\int dt\,(6\textstyle\sum_i I_i^2+8\sum_{i,j}' I_iI_j) . \qquad (4.15)$$

This quantity is not simply a multiple of F_0, as are F_p and F_b.

Before proceeding to simplify Eq. (4.14), we prove our contention that the term $S(\tau)$ given by Eq. (4.14) is negligible in the middle region. We write $\mathcal{E}_i$ and $\mathcal{E}_{Ri}$ as slowly varying amplitudes multiplied by complex exponentials,

$$\mathcal{E}_i(z,t)=\mathcal{V}_i(z,t)e^{-i(k_iz+\Omega_{ci}t)}$$

and $\mathcal{E}_{Ri}(z,t)=-\mathcal{V}_i(z,t-\tau)e^{i(k_iz-\Omega_{ci}t)}$,

where $k_i=\Omega_{ci}/v_i$. Letting $\mathcal{V}_i\equiv\mathcal{V}_i(z,t)$ and $\mathcal{V}_{Ri}\equiv-\mathcal{V}_i(z,t-\tau)$, one obtains for the amplitude correlation function

$$G_i=\mathcal{V}_i^*\mathcal{V}_{Ri}e^{2ik_iz}=\mathcal{V}_i^*\mathcal{V}_{Ri}e^{i\Omega_{ci}\tau}$$

and, consequently,

$$S(\tau)=\sum_{i,j}{}'\mathcal{V}_i^*\mathcal{V}_{Rj}^*\mathcal{V}_{Ri}\mathcal{V}_je^{i(\Omega_{ci}-\Omega_{cj})\tau} .$$

To examine the behavior of this function near $\tau=0$, that is, for

$$\tau\ll 2\pi/m_i\Delta\Omega_i, \quad (i=1,\ldots,M)$$

we let $\mathcal{V}_{Ri}=-\mathcal{V}_i$. If we assume that each group contains the same number of modes,

$$m_i=m_g\equiv m/M, \quad (i=1,\ldots,M) ,$$

all of equal intensity w and with the same spacing, $\Delta\Omega_i=\Delta\Omega$, then we have

$$S(\tau)=m_g^2w^2(\,|\sum_{l=-N}^{N}e^{ilm_g\Delta\Omega\tau}|^2-M)$$

$$= m_g^2 w^2 \left(\frac{\sin^2(\frac{1}{2}m\Delta\Omega\tau)}{\sin^2(\frac{1}{2}m_g\Delta\Omega\tau)} - M \right). \qquad (4.16)$$

The width τ_s of this function is given by $\tau_s = 2\pi/m\Delta\Omega$, as was surmised. Note that Eq. (4.16) has the form of an M-beam interference function with a second peak equal in height to the peak at $\tau = 0$ when $\tau = 2\pi/m_g\Delta\Omega = M\tau_s$. However, for such large values of τ our assumption that $v_{Ri} = -v_i$ is not valid. If we take into account the variation of v_{Ri} with τ, this peak is drastically reduced in amplitude. Moreover, if we allow the groups to contain unequal numbers of modes, the subsidiary peaks are washed out altogether. We will see an illustration of this effect later (Fig. 10).

Now we turn to the reduction of Eq. (4.15) for the fluorescence in the middle region, assuming that each of the M groups contains m_g modes having intensity w and spacing $\Delta\Omega$. Then I_i is given by the squared modulus of Eq. (4.4), and the fluorescence reduces to

$$R_m \equiv F_m \big| F_0 = 4 + 2(2M-1)^{-1} .$$

This ratio plunges rapidly from 6 down to 4 as the number M of groups increases. For example, for $M = 11$ we already have $R_m = 4.1$.

When there is only one group of modes ($M = 1$), the middle region vanishes and the above results reduce to those for the perfect-locking case.

An important consideration in this model is that the width of the sharp central peak with contrast ratio $R = 3$ relative to the background is characteristic of the width of $S(\tau)$, that is the inverse spectral width or the coherence time $\tau_c = 2\pi/m\Delta\Omega$, and bears no relation to the pulse width. On the other hand, the width of the middle plateau, with a contrast ratio of about 2 relative to the background, is a measure of the pulse width $\Delta t \cong 0.88\pi/m_g\Delta\Omega = M\tau_c$.

We turn to the computer again to illustrate some of our results and check the approximations involved. Moreover, the computer will allow us to calculate the detailed shape of the TPF profiles. The assumption that the large number of modes is ordered into a relatively small number of domains allows us to use an analytic expression for the domain amplitudes, thus making the computer solution feasible. We use the same parameters introduced above to illustrate the behavior of the intensity. The results for the domain model are to be compared to those for the perfectly locked laser, shown in Fig. 7(b). The TPF relative to the single-pass fluorescence $F(\tau)/F_0$ is plotted[31] as a function of the time delay τ. The result is a curve which drops smoothly from the peak value $F/F_0 = 6$ to the background value $F/F_0 = 2$ in a time (half-width at half-maximum) $\tau = 0.22$ psec, in agreement with our expectations.

Returning to the domain model, we show the TPF curve in Fig. 8 corresponding to the two sample functions of Fig. 5. One notes in each case a sharp central peak with contrast of 6 relative to the single pass, followed by a plateau of mean contrast starting near 4 which falls off nonmonotonically to the background level of 2. The fluorescence in the middle region is a smoother function than the intensity, as one would expect since it is a convolution of the intensity; however, there still are prominent random wiggles varying from sample to sample. The wiggles disappear when the TPF from several sample functions is superposed, as indicated by Fig. 9. This figure shows a crude Monte Carlo estimate for the TPF resulting from 60 pulses with different sets of random phases $\{\varphi_{ci}\}$. The random phases chosen are the ones used to compute the intensity of Fig. 6; however, the curve is *not* the same as would be obtained from a single pulse whose intensity is given by Fig. 6. The reason is simply that the single-pass fluorescence F_0 will vary from one sample function to another, even though the total energy in the pulse remains constant. As a result, the correct way to compute the fluorescence is to sum separately the fluorescence at τ from each pulse and the single-pass fluorescence from each pulse and then take the ratio. By contrast, computing the TPF from Fig. 6 is equivalent to performing the division on the individual sample results before summing.

The TPF curve of Fig. 9 shows clearly the sharp central component and a broad plateau falling off to the background of half-width $\tau = 2.25$ psec (measured at the level $F/F_0 = 3$). Most of the structure in the plateau region has been smoothed out, with the notable exception of a subsidiary peak near $\tau = 4.1$ psec. This peak is not a vestigial fluctuation due to poor convergence, but

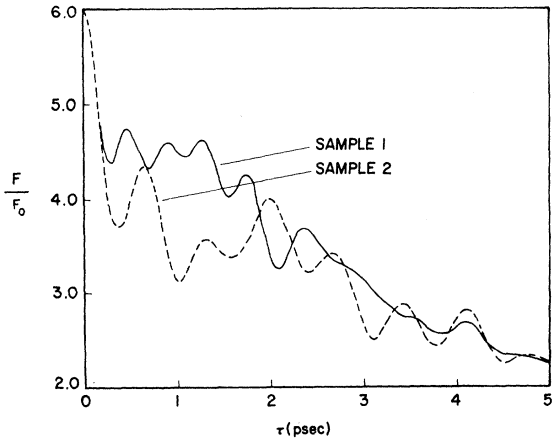

FIG. 8. Relative TPF yield $F(\tau)/F_0$ in the domain model for the two samples of Fig. 5.

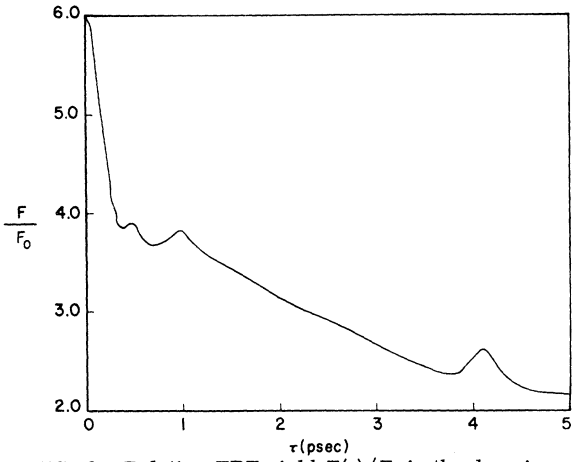

FIG. 9. Relative TPF yield $F(\tau)/F_0$ in the domain model for the sum of 60 samples. Parameters are the same as in Fig. 5.

rather is the secondary peak of the function $S(\tau)$ of Eq. (4.14) referred to above. From the discussion following Eq. (4.16) we conclude that this peak should occur at 11 times the inverse spectral width of 0.376 or 4.1 psec, in good agreement with Fig. 9. To suppress the secondary peak, we need only make the beats between the various mode groups reach their maxima at different values of τ. This is achieved by making the groups unequal in size, an assumption more likely to correspond to real lasers than that of equal-size groups. In Fig. 10 we show $F(\tau)/F_0$ resulting from the sum of 10 pulses corresponding to different sample functions for this case, where indeed the smaller peak has disappeared. The convergence also appears to be considerably more rapid in this case than in that of equal-size groups.

V. DISCUSSION

In this final section we compare the above theoretical results with experiment and conclude that the partial-locking model, as an explanation of low contrast ratios, is in direct contradiction with existing experimental data in several respects while the domain model is in reasonably good agreement with them. We then examine briefly the dynamical foundations of the domain model, pointing out some deficiencies. Finally, we note certain general features required of any model of an imperfectly mode-locked laser which hopes to explain the experiments.

A. Comparison with Experiment

The partial-locking model is incompatible with experiment for at least two reasons. The first is that, for realistic values of the mode number m and the parameter β, this model cannot simultaneously yield the low values of the peak-to-background TPF contrast ratio R and the high peak-to-background photocurrent intensity ratios r seen experimentally.[32] For example, referring to Fig. 4, we note that for $\beta = 40$ (corresponding to a cavity round-trip time of $t_{\text{pulse}} = 10$ nsec and a detector response time $T_d = 0.25$ nsec) and $m = 26\,600$, one requires $r \cong 2$ to reduce R to 2.0; that is, one requires a peak on the oscilloscope trace only three times the background noise level. Even for $m = 530$ one has $r \cong 4$. On the other hand, we note that several authors[7,25] have reported values of R close to 2, while failing to find any measurable background radiation at all,[33] although their experiments should be able to detect values of r perhaps as high as 50.

The second reason for rejecting the partial-locking model is that it achieves lower values of R by increasing R_b above 2.0, whereas experiment[5] shows that R_b remains approximately 2 and that the low value of R is due to a decrease of R_b.

On the other hand, we find that the domain model compares much more favorably with experiment than does the partial-locking model. We have $R_b = 2.0$ and r virtually infinite for any reasonable parameters in agreement with the photodiode-oscilloscope measurements and with the background-to-single-pass TPF contrast measurements. Moreover, Shapiro and Duguay[34] have performed an experiment with cleanly mode-locked Nd-glass laser pulses, using a thin (28μ) dye cell moved along the overlapping beams and recording the TPF photoelectrically, which is in agreement with the domain model. In particular, the experimental points in the fluorescence curve of their Fig. 2 are consistent with the general shape of our Figs. 9 and 10. Whereas for a single structureless pulse, one would expect the

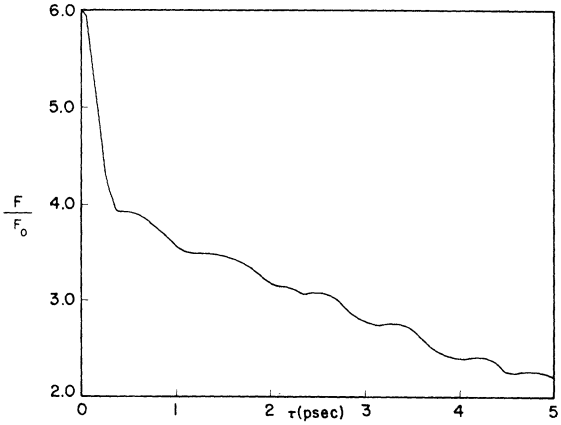

FIG. 10. Relative TPF yield $F(\tau)/F_0$ from 10 samples in the domain model for mode groups of unequal size. Parameters are same as in Fig. 5, except that the number of modes m_i in the ith group satisfies $m_i = m_6 e^{-\alpha|i-6|}$ with α chosen so that $m_1/m_6 = m_{11}/m_6 = 0.5$.

fluorescence curve to be about twice as wide at the level $F/F_0 = 5$ as at the level $F/F_0 = 3$ [see Fig. 7(b), for example], the Shapiro-Duguay data indicate a ratio of 10 to 15 between these widths. This indicates the existence of two components to the trace: a sharp central component (maximum contrast 3 relative to the background) and a broader plateau (maximum contrast 2 relative to the background). It is not clear why the photographic records of the usual experiments perfomed with thick dye cells (indicated in Fig. 1) do not show this same sharp peak with $R_p = 6$. However, the fact that the discrepancy between the usual and the thin-cell method persists when both experiments are performed on the same laser[35] leads one to suspect that the sharp central peak is real and does not appear in the usual thick-cell experiment due to some undetermined peculiarity of the method.[36,37]

Several comments on the experimental situation can be made on the basis of the above discussion.

(i) Klauder and Weber correctly point out the importance of *quantitative* results in using the TPF method to determine whether a laser is emitting picosecond pulses and, if so, what their characteristics are. Nevertheless, it is not generally realized that measurements of R_p and R_b are much more reliable indicators of the nature of the laser radiation than is a measurement of R. In fact, the existence of regularly spaced regions where $F/F_0 = 2$ is a clear indication that one has a train of sharp pulses, since these must be background regions where there is no overlap between E and E_R. This information is especially useful when the mode spacing is so large that the pulses cannot be resolved by a photodetector.[2,38] If such background regions exist, the width of one of the regions where $F/F_0 > 2$ is then a direct measure of the pulse width, regardless of its contrast relative to the background. If the spacing in τ between regions of enhanced fluorescence is greater than T_d, a simultaneous display of the photocurrent on an oscilloscope should show a train of pulses with 100% modulation. On the other hand, if there are no regions where $F/F_0 = 2$, then there must be a continuous noise component to the laser emission (partial locking). As the mean intensity of the noise increases from 0 to 100% of the total (η_l decreases from 1 to 0), R_b increases from 2 to 4.

(ii) It is clear from Figs. 8–10 that it is important to take densitometer traces of the fluorescence for a sufficiently large range of τ, especially if one does not measure F_0. Otherwise, one could easily miss the broad plateau, confusing it with the background, and think that the sharp central peak represents the pulse width. Ideally, both a fast detector (TPF dye) and a slow detector (photodiode-oscilloscope) should be used, and the range of values of τ examined with the fast detector should be at least as great as the resolution time of the slower one.

(iii) A measurement of the spectrum of the laser radiation, concurrently with the TPF experiment, is of great importance because it provides one with information necessary to pick a model for the laser radiation, such as the value of m and the time-bandwidth product corresponding to various regions of the TPF display. If the time-bandwidth product for the region where $F/F_0 > 2$ is unity, then only intensity fluctuations are present. On the other hand, if the product exceeds unity, there are also phase fluctuations. To obtain information about the character of the phase fluctuations (for example, whether they are systematic or random), one can pass the radiation through a dispersive element and examine the TPF as a function of the dispersion,[11] or one can pass the radiation through a Michelson interferometer before allowing it to enter the TPF apparatus.

(iv) Time-resolved measurements of spectra and TPF traces would be valuable in ascertaining the extent to which phase diffusion occurs in the evolution of the laser pulse train by comparison with time-integrated measurements. For example, in regard to the domain model, one could determine whether the individual sample results of Fig. 8 or the ensemble-averaged results of Figs. 9 and 10 agree more closely with experiment.

Of course, the domain model is not the only conceivable model capable of yielding TPF traces in accord with the Shapiro-Duguay results. Nevertheless, we feel that the domain model is worthy of detailed study because it is simple enough to enable one to make detailed analytic and computer calculations readily, as seen in Sec. IV, and also because one can cite heuristic dynamical arguments in its favor. We discuss the latter point next.

B. Dynamical Considerations

On the basis of the steady-state theory of laser operation, one can make a very plausible, although still heuristic and tentative, argument for the domain model. Following Statz,[25,39] we view the problem of determining the extent of mode locking as one of evaluating the competition between two opposing tendencies. One is the deviation from linearity of the dispersion relation which causes mode spacings to be unequal, thus preventing their phases from locking; the other

is the generation of nonlinear-polarization sidebands due to the mode interaction which act as external signals tending to quench the nearby natural oscillations and to replace them by equally spaced driven oscillations. If the sidebands generated in the saturable absorber are only sufficiently intense to lock modes whose frequency differences vary by a limited amount (the locking range[40]) which is small compared to the spectral width, the result may be a series of groups of locked modes, as in the domain model.

This process may be illustrated by reference to Fig. 3 of Ref. 39, which can be considered, for our purposes, to be a hypothetical anomalous dispersion curve. The vertical scale shows the difference between the empty-cavity resonance frequency and the corresponding frequency in the cavity containing the amplifying medium and the saturable absorber. The horizontal scale shows the wave vector k referred to its value at the center of the gain curve. The process of perfect locking consists of replacing the dispersion curve by a single straight line, as shown. On the other hand, the domain model is a consequence of fitting the dispersion curve with a series of line segments. The amount of phase adjustment required is considerably less than for perfect locking. Consequently, locking into domains could result when the nonlinear-polarization driving terms are too weak to lead to perfect locking.

As discussed in Sec. IV, each group of locked modes will form a pulse. In general, one might think, the pulses corresponding to the various groups will not coincide in time, resulting in several circulating pulses per cavity round-trip time. This could be achieved by allowing the phases of the lowest-frequency beat notes in each group [φ_i in Eq. (4.5b)] to be different. In practice, however, it will clearly be energetically advantageous for the various pulses to pass through the dye nearly simultaneously,[41] the field being required then to open a window of transparency in the dye only once per round trip.

If one recalls our discussion of locking in terms of nonlinearity of the dispersion law, a problem appears in connection with the synchronization of the pulses corresponding to the several groups. Because the straight-line segments used to fit the dispersion law have different slopes, the group velocities of the corresponding pulses will differ. Thus, if the pulses overlap at one time, they will cease to overlap sometime later. However, the amount by which the pulses disperse during the duration of the Q-switched pulse is very small. Assuming a reasonable number for the maximum deviation from equidistant frequency spacing to be expected (~ 1 MHz) and a pulse duration of 500 nsec, one finds that the peaks will shift by about 0.3 psec. This shift will cause a change in the detailed substructure within a single mode-locked pulse (and, consequently, also in the details of the TPF) during the evolution of the pulse train, but is too small to cause the pulse to split up.[42]

There is, however, a more basic difficulty with this quasi-steady-state argument for the domain model. This is the fact that mode locking in solid-state lasers is a transient phenomenon. Although the steady-state theory has been quite successful in dealing with many locking phenomena in cw gas lasers[43] and although many investigators have assumed its relevance to the pulsed solid-laser case and even performed calculations based on this assumption,[39,25,44] we are aware of no argument pretending to justify this assumed applicability. In fact, we believe that this type of theory may have little bearing on solid-laser mode locking and that a dynamical justification of the domain model (or of any other model, for that matter) requires that one consider the transient problem. This is a subject of current investigation. There is reason to believe that a viable argument for the domain model can still be formulated.

C. General Remarks and Conclusion

So far we have not mentioned the behavior of the phase $\Phi(z,t)$ of the electromagnetic field in the domain model. In general, not only the intensity but also the phase will fluctuate randomly within a single pulse. Although the TPF technique is insensitive to phase fluctuations, passing the field through a dispersive delay line will result in some FM-to-AM conversion, so that a subsequent TPF experiment will yield information on the phase of the original field. Using such an apparatus Treacy[11] claims to have found a systematic quadratic time dependence of Φ, resulting in a linear frequency sweep or "chirp." An alternative explanation of his results, allowing for the possibility mentioned above of confusing the plateau region with the background, is that an initial pulse with random phase fluctuations and very weak intensity fluctuations is converted by the dispersive element into one with appreciable intensity fluctuations. We point out here that such results could occur occasionally in the present model through statistical fluctuations.[45] Just as certain choices of $\{\varphi_{ci}\}$ yield fields with negligible phase variations and nearly minimum-duration pulses, so other choices yield fields with strong systematic or random phase variations and weak intensity variations. Moreover, the likelihood of such choices for the phases could be enhanced by as yet unknown dynamical effects.[46]

In conclusion, we have demonstrated that the partial-locking model is incompatible with present experimental evidence on the type of imperfect mode-locking occurring in solid (especially Nd-glass) lasers and that the domain model agrees rather well with it. Because our discussion of the partial-locking model has not relied heavily on the details of the model, but only on the break-up of the field into a coherent part, occurring as a train of short pulses, and a chaotic part, appearing as a fluctuating background, we can add that no other model[10] in which the deviations from perfect locking are such as to result in a uniform background, can explain the experimental results. Rather, the types of deviations from perfect locking compatible with experiment are those which do not destroy the sharpness and disjointness of the field pulsations. The domain model is a plausible model incorporating such compatible deviations.

In this regard note that there is considerable latitude for change within the domain model without negating its underlying insights. The basic idea is that one assumes the mode phases to vary linearly over considerable portions of the oscillating spectrum, resulting in a field $\mathcal{E}$ made up of several components $\mathcal{E}_i$, each of which is a short pulse corresponding to near-perfect locking. One may then regard each perfectly locked set of modes as a "supermode" out of which a general pulsed field can be constructed. In the above discussion we have assumed that the relative phases of the supermodes or domains are random over the range $(0, 2\pi)$ for lack of any compelling empirical or dynamical grounds for making another ansatz. However, many other choices for the group phases are possible, just as one can choose the phase differences of the individual modes in many different ways. In particular, (a) the phases φ_{ci} can be assumed to have undergone a random walk and achieved some distribution over a range $(-f, f)$ about their initial values in order to account for a degree of partial phase averaging over the ensemble occurring in a particular experiment; (b) they can be chosen to yield a randomly varying phase with negligible intensity fluctuations, or vice versa; (c) they can be chosen to yield systematic phase variations, resulting in a frequency sweep.

---

[1]A. J. DeMaria, W. H. Glenn, Jr., M. J. Brienza, and M. E. Mack, Proc. IEEE 57, 2 (1969).

[2]J. A. Giordmaine, P. M. Rentzepis, S. L. Shapiro, and K. W. Wecht, Appl. Phys. Letters 11, 216 (1967).

[3]The TPF technique has the considerable advantage of requiring only a single firing of the laser, in principle, to obtain a display of the entire intensity-correlation function.

[4]H. P. Weber, Phys. Letters 27A, 321 (1968); H. P. Weber and R. Dändliker, J. Quantum Electron. 4, 1009 (1968).

[5]J. R. Klauder, M. A. Duguay, J. A. Giordmaine, and S. L. Shapiro, Appl. Phys. Letters 13, 174 (1968).

[6]H. E. Rowe and T. Li [J. Quantum Electron. 6, 49 (1970)], present exhaustive calculations on both of these models.

[7]G. Kachen, L. Steinmetz, and J. Kysilka, Appl. Phys. Letters 13, 229 (1968).

[8]R. J. Harrach, Phys. Letters 28A, 393 (1968); Appl. Phys. Letters 14, 148 (1969).

[9]R. H. Picard and P. Schweitzer, Phys. Letters 29A, 415 (1969).

[10]A. A. Grütter, H. P. Weber, and R. Dändliker, Phys. Rev. 185, 629 (1969). This paper also contains an exhaustive list of references to which the reader is referred.

[11]E. B. Treacy, Phys. Letters 28A, 34 (1968).

[12]R. J. Glauber, Quantum Optics and Electronics, edited by C. DeWitt, A. Blandin, and C. Cohen-Tannoudji (Gordon and Breach, New York, 1965), p. 63.

[13]B. R. Mollow, Phys. Rev. 175, 1555 (1968).

[14]This assumption is always true when the fluorescence is monitored photographically. On the other hand, when the recording device is a phototube, it may be possible to make time-resolved fluorescence measurements. Yet no such measurements have been reported.

[15]This result is also in Weber, Ref. 4.

[16]L. Mandel and E. Wolf, Rev. Mod. Phys. 37, 231 (1965).

[17]In the quantum theory of coherence the analytic signal appears naturally as the eigenvalue of the field annihilation operator $E^{(+)}$, defined by the relation $E^{(+)}(z, t)|\ (z,t)\rangle = (z,t)|\ (z,t)\rangle$. See Refs. 12 and 16.

[18]One often chooses instead a superposition of complex amplitudes with fixed modulus but uniformly distributed over-all phase Φ'. The resulting distribution, $P(\{\epsilon_k\}) = (2\pi)^{-1}\int_0^{2\pi} d\Phi'\, \delta[\mathcal{E}(z,t) - \mathcal{E}'(z,t)e^{i\Phi'}]$, has the property of stationarity, which is desirable in some instances, but only obscures the basic problem here.

[19]The derivation of Eq. (2.8) depends on whether m is even or odd. For example, when $m = 2n+1$, one substitutes $\Omega_k = \Omega_c - k\Delta\Omega$ and $\epsilon_k = w^{1/2}\exp[i(\varphi_c - k\varphi)]$ into Eq. (2.5) and lets the index k vary over the range $-n$ to n. A different substitution is necessary when m is even.

[20]To demonstrate this for the second-order correlation functions of interest to us, substitute Eq. (2.5) into Eqs. (2.4). The integrations can then be carried out easily by making use of the constancy of the individual mode amplitudes and the uniformity of the distribution of each modal phase. The resulting expression for $G^{(1)}$ varies as m and that for $G^{(2)}$ as $m(m-1)$. The terms in $G^{(2)}$ of order m^2 can be expressed in terms of $G^{(1)}$ so that the expression for $G^{(2)}$ takes the form of Eq. (2.13), with a term left over of order m. This shows the nearly Gaussian nature of the statistics and the mag-

nitude of the deviation from Gaussianity.

[21]For a similar discussion in connection with harmonic generation, see J. Ducuing and N. Bloembergen, Phys. Rev. 133, A1493 (1962); and N. Blembergen, *Nonlinear Optics* (Benjamin, New York, 1965), p. 131.

[22]The result is obtained easily if one makes an envelope approximation, replacing $E^{(+)}(z,t)$ by a complex carrier $e^{-i(k_c z+\Omega_c t)}$ times an amplitude $V(z,t)$ which varies slowly in space and time on an optical scale.

[23]There is no need to distinguish the spatially averaged fluorescence from the unaveraged fluorescence in the single-pass case. Since the field now consists of traveling waves, there is no optical frequency variation with τ.

[24]This relation is approximate because it ignores the effects of the small mode-frequency shifts due to the interaction with dispersive elements in the cavity (including the active medium and the saturable absorber) and it ignores the widths of the individual modes due to spontaneous-emission noise.

[25]This model was suggested to the authors by some remarks by H. Statz and M. Bass, J. Appl. Phys. 40, 377 (1969).

[26]In Ref. 9 the integrand of Eq. (3.10a) was approximated by a rectangular function of height $(m_l W_l)^2$ and width $2\pi/m_l\Delta\Omega$, so that the value of F_{ol} used was 1.5 times larger than the present value.

[27]R. A. Bradbury (private communication).

[28]This value is 0.44 times the half-width to the first zero (the inverse spectral width).

[29]Assume a rectangular pulse for simplicity.

[30]Contrary to the case of TPF, it does matter whether one changes m by keeping $\Delta\Omega$ constant or by keeping the bandwidth $m\Delta\Omega$ constant. Only the former will leave r invariant, because β is a function of $\Delta\Omega$.

[31]In this figure and the following ones, F is only plotted for positive values of τ because the curve is symmetric about $\tau=0$. This symmetry about the zero-delay position is present in a TPF experiment whenever the fields E and E'_R traveling in opposite directions through the fluorescing dye are identical.

[32]Of course, many workers have seen obvious cases of partial locking, in which the oscilloscope trace consists of pulses on a continuous background [for example, A. J. DeMaria, D. A. Stetser, and W. H. Glenn, Jr., Science 156, 1557 (1967)], without reporting TPF contrast ratios. We specifically exclude such cases from consideration here and confine ourselves to cases where we have some reason to believe that the laser output consists of well-defined pulses, such as a clean oscilloscope trace.

[33]The contention by Harrach (Ref. 8) that the partial-locking model allows low values of R while maintaining clean oscilloscope traces of the photodiode output is based on two factors: (i) An unreasonably small number of modes ($m=100$) is chosen, and the mode-number dependence of R is overlooked, and (ii) the finite response time T_d of the detector, which reduces the prominence of the photocurrent peak relative to that of the intensity peak, is neglected.

[34]S. L. Shapiro and M. A. Duguay, Phys. Letters 28A, 698 (1969).

[35]A. R. Clobes and M. J. Brienza, Appl. Phys. Letters 14, 287 (1969).

[36]That the resolution of the method is sufficient to see the sharp peak is confirmed both by theory (Ref. 2) and by the fact that such small-scale structure has been observed in other circumstances. [See Ref. 11 and also D. J. Bradley, G. H. C. New, B. Sutherland, and S. J. Caughey, Phys. Letters 28A, 532 (1969).] Nevertheless, the observation should require considerable care in alignment, and it is possible that the peak has been overlooked.

[37]Since this manuscript was completed, photographic observation of a sharp central component in a thick-dye cell has indeed been reported by D. J. Bradley, G. H. C. New, and S. J. Caughey, Phys. Letters 30A, 78 (1969).

[38]M. A. Duguay, S. L. Shapiro, and P. M. Rentzepis, Phys. Rev. Letters 19, 1014 (1967); S. L. Shapiro, M. A. Duguay, and L. B. Kreuzer, Appl. Phys. Letters 12, 36 (1968).

[39]H. Statz, J. Appl. Phys. 38, 4648 (1967).

[40]C. L. Tang and H. Statz, J. Appl. Phys. 38, 323 (1967).

[41]This conclusion seems to be a straightforward consequence of the maximum-emission hypothesis, for example [C. L. Tang and H. Statz, J. Appl. Phys. 38, 2963 (1967); S. E. Schwartz and P. L. Gordon, J. Appl. Phys. 40, 4441 (1969).]

[42]Of course, it is also too small to account for the pulse lengthening from 8 to 15 psec during the pulse train seen by some [W. H. Glenn, Jr., and M. J. Brienza, Appl. Phys. Letters 10, 221 (1967)].

[43]For example, W. E. Lamb, Jr., Phys. Rev. A134, 1429 (1964); H. Statz, G. A. de Mars, and C. L. Tang, Appl. Phys. Letters 14, 125 (1969); and H. Statz, G. A. de Mars, and C. L. Tang, Appl. Phys. Letters 15, 428 (1969).

[44]S. E. Schwartz, J. Quantum Electron. 4, 509 (1968).

[45]Since the number of random variables (M) is reasonably small, the probability of such atypical fluctuations is reasonably high.

[46]Multiphoton absorption and various types of stimulated scattering, for instance, are known to inhibit amplitude fluctuations, and their occurrence in some mode-locked lasers is perhaps not ruled out.